Time Correlation Properties Of Dynamic Mobile To Mobile Channels In Indoor Environments

Gloria Makhoul[1,2,3], Francesco Mani[1,2], Raffaele D'Errico[1,2], Claude Oestges[3]
[1]CEA-LETI, Grenoble, France
[2]Université Grenoble-Alpes, Grenoble, France
[3]ICTEAM Electrical Engineering, Université catholique de Louvain (UCL), Louvain-la-Neuve, Belgium
Email: {gloria.makhoul, francesco.mani, raffaele.derrico}@cea.fr, claude.oestges@uclouvain.be

***Abstract*—This paper analyzes the temporal correlation properties of mobile-to-mobile (M2M) channels, based on an extensive measurement campaign carried out in an indoor environment at 2.48 GHz. In order to model the dynamic channel characteristics, short- and long-term fading behaviors are extracted. The auto-correlation function (ACF) is characterized for different types of pedestrian movements. Finally the results of a channel model implementation preserving the ACF properties are presented, showing good match with those obtained from measurements.**

***Index Terms*—Mobile-to-Mobile channel, indoor, correlation.**

I. Introduction

Mobile-to-mobile (M2M) wireless communications occur when both transmitter and receiver are moving in the environment. In Intelligent Transport Systems (ITS) and ad-hoc networks, the mobile terminals are often cars and, therefore, communication takes place between two vehicles. However, the mobility can arise from the pedestrians carrying wireless nodes communicating, as a part of Device-to-Device (D2D) communication. A particular subset of these networks is given by multiple Body Area Networks (BANs) coexisting and cooperating in the same environment.

The characteristics of the M2M channels are quite different from classical Fixed-to-Mobile (F2M) channels and they request the development of specific models. However, most of the research activities have focused on M2M channel models for outdoor environments, by means of real-world measurements and simulations, e.g. ray tracing, whereas the number of contributions dedicated to indoor premises has been rarely addressed in the literature.

The mobile indoor peer-to-peer radio channels were presented in [1], where multiple fading distributions depending on the mobility of the nodes and on the environment itself were investigated. The cooperative indoor-to-indoor and outdoor-to-indoor radio channels were studied at 2.4 GHz in [2]. The shadowing correlation between different point-to-point links was presented there as an exponentially decay law, where a high shadowing correlation was revealed due to node mobility. Moreover, a low shadowing correlation between antennas distributed on human body was exhibited in [3] and a diversity scheme was implemented in order to mitigate the body shadowing. An indoor body-to-body (B2B) narrow-band channel model at 2.45 GHz was presented in [4], where the dynamic properties of the channel were studied for different communication conditions according to the mutual position of the subjects and their corresponding movements. The fading channel for single or multiple antenna body-worn system was found to be well described by a $k-\mu$ distribution in an indoor environment for firefighters deployment scenarios in [5]. The results were obtained from analysis of experimental data collected indoor at 2.45 GHz when users perform some random walking movements. Furthermore, a stochastic differential model for M2M channel was developed in [6] and it was tested experimentally in indoor and outdoor environments. This model estimated the statistics and the time variation of the channel based on the received signal.

Concerning the characterization of time correlation properties of M2M channels in indoor environment, contributions were presented in [2], [3], [5]. Although multiple M2M temporal correlation models were developed for different outdoor scenarios in [7]–[9], according to the knowledge of the authors non one of them have been applied on indoor M2M scenarios until now.

Hence, in this paper, we exploit an extensive B2B measurement campaign in an indoor environment in order to extract the auto-correlation properties of the channel. In particular, we focus our analysis on the channels where the antennas were mounted at both sides of the helmet of different people. This was done to minimize the effects of body shadowing in order to extend our evaluations from B2B specifically towards a more general M2M scenario. Our goal is to present a comparison of auto-correlation functions between several types of movements both for long- and short-term fading and to derive a channel model implementation able to reproduce such characteristics.

This paper is organized in the following way. A brief description of the measurement campaign and the data post-processing are provided in Section II. Section III compares the auto-correlation functions (ACF) of the dynamics channel characteristics. Then, it presents an implementation using the Cholesky factorization on the second order fading statistics in order to generate stochastic processes which can describe the channel characteristics. Finally, the conclusion is given in Section IV.

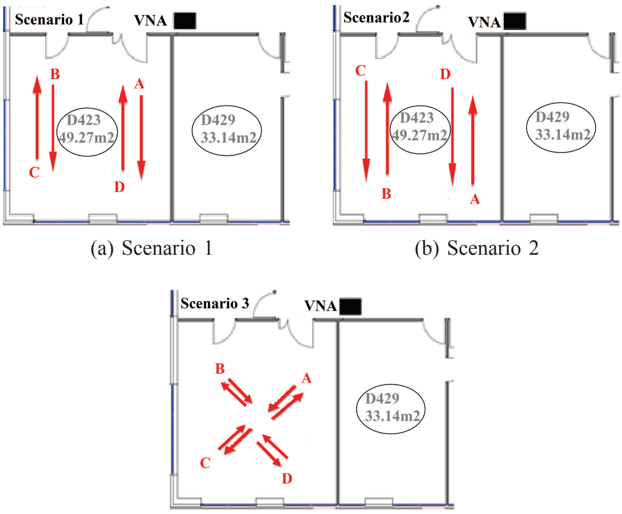

(a) Scenario 1 (b) Scenario 2

(c) Scenario 3

Fig. 1. Visual plan of measurement scenarios, including walking patterns

II. M2M Indoor Channel Characterization

A. Measurement Campaign

A narrow-band channel measurement campaign was carried out in an office environment at CEA Leti at 2.48 GHz [10]. The measurement campaign included various indoor locations, e.g. single and multiple rooms, as well as multiple antennas positions on the user, e.g. head, wrist and belt. The results here presented focus on a single room scenario and a simple monopole antenna which was mounted vertically on the right side of a helmet placed on the head of the moving subject. Four people were simultaneously in the same room, a 49 m^2 classical office with desks, storage cabinets and bookshelves. During measurements, furniture was arranged at the sides of the room leaving a large empty part in the center where the subjects were moving during the measurements. A 4-port Vector Network Analyzer (VNA) was employed to record full S-matrix of the measurements.

Multiple human mobility scenarios were considered in the measurements. In this work, we focus on straight line walking scenarios, including parallel, opposite and cross walk as described in Fig.1 and Table I. A, B C and D represent the four different subjects involved in measurements. The duration of each measurement acquisition was 10 s and people were moving at a constant speed of approximately 0.5 m/s. A sonorous synchronization was used in order to aid the subjects to move at a regular pace. Measurements were recorded each 4 ms, providing 2501 samples for each link.

B. Channel Modeling Approach

The outcome of the measurements is the instantaneous narrow-band channel response over time $H(t)$. In post-processing, it was decided to separate Path-Loss (PL), mainly due to distance between mobiles, from the long-term and short-term fading. Hence, the time-variant channel power can

TABLE I
Types Of Walking Movements

Realization	Scenario number	Walking pattern
AB and CD	1-2	Parallel walk
AC and BD	1-2	Far opposite walk
AD and BC	1-2	Opposite walk
AB and CD	3	Toward and back walk 1
AC and BD	3	Diagonal walk
AD and BC	3	Toward and back walk 2

be expressed as:

$$|H(t)|^2 = PL(t)^{-1} \cdot S(t) \cdot |F(t)|^2 \tag{1}$$

where $F(t)$ and $S(t)$ represent short-term fading and long-term fading, respectively.

Short-term fading is extracted from measurements by filtering the acquired data with a time domain rectangular sliding window of 0.5 s. Filtering was performed on the channel envelop in linear scale. Long-term fading is separated from what is left after short-term fading subtraction, by deriving a PL law. Generally, the PL is described as a function only of the distance d. However, in [11] it was shown that in B2B scenarios it also depends on the mutual orientation between the bodies, α, as result of body shadowing. Accordingly, it can be written, in dB, as:

$$PL(d,\alpha) = PL_0(\alpha) + 10n\,(\alpha)\,log(\frac{d}{d_0}) \tag{2}$$

where PL_0 and n are the losses at the reference distance d_0=1m and the path loss exponent, respectively. The dependence on mutual orientation is not significant in the type of channel we investigate in this paper as antennas on head position are not significantly influenced by body shadowing.

Therefore, also long-term fading reflects the variation in the average received power due to macro-effect caused by furniture presented in the environment and not body shadowing. It is classically described by log-normal distribution and, in our scenario, it is characterized by a variance of 1.8 dB, on average.

Short-term fading characterizes the fluctuations of the received signal over short distance, given by the multipath propagation. In [10], it was found that, for B2B channels with significant body shadowing, the short-term fading can be described by a Rician distribution whose K-factor is a function of α. However in head-to-head channels also this angular dependence can be neglected. Therefore, an average K-factor of 2 has been found.

III. Time Correlation Properties Analysis and Modeling

In this section, we present the time correlation properties of the normalized transfer function, long-term fading and short-term fading. We considered the normalized transfer function as the complex transfer function $H(t)$ of the channel normalized with respect to its PL.

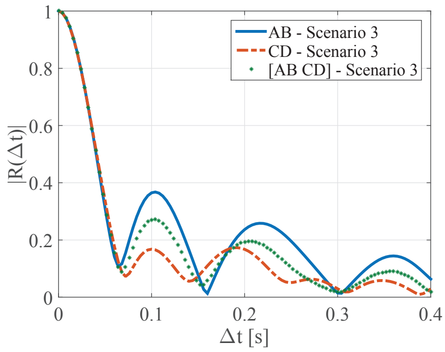

Fig. 2. ACF of short-term fading component for towards and back walk 1 scenario

TABLE II
COHERENCE TIMES

	Coherence time (ms)		
Walking pattern	*Normalized transfer function*	*Short-term fading*	*Long-term fading*
Parallel walk	34.7	34.2	529.9
Opposite walk	20.9	20.7	537.4
Towards and back walk 1	30.3	29.2	1103

If we consider a given scenario and similar mobility patterns, we can assume for simplicity that the M2M channel is a wide sense stationary (WSS) channel, thus the normalized ACF can be expressed in the following way [12]:

$$R(\Delta t) = \frac{E\left[X(t) \cdot X^*(t+\Delta t)\right]}{\sqrt{E\left[|X(t)|^2\right] \cdot \sqrt{E\left[|X(t+\Delta t)|^2\right]}}} \tag{3}$$

where $X(t)$ is a stochastic process that represents either the short- or long-term fading or the normalized transfer function.

It is important to note that the long-term fading ACF is computed over its values in dB scale, while the channel transfer function and short-term fading ACFs are computed over complex values in order to study the impact of the phase information.

A. Measurement Results

As a first step, we compute the ACF for each channel and for each specific acquisition. Fig. 2 shows the comparison of short-term fading ACFs for different realizations and a given type of walking, i.e the toward and back walk 1. It can be noticed that regardless of the specific acquisition, the ACF patterns are qualitatively similar. It is thereby relevant to aggregate together all data samples of realizations with the same walking pattern.

Figs. 3, 4 and 5 present the ACFs of the long-term fading, the short-term fading and the normalized transfer function for three of the walking patterns described in Table I. Table II presents the coherence time at 0.7 of the ACF for each walking scenario and channel characteristics.

As expected, the long-term fading presents the higher coherence time. The ACF can be modeled, as a first approximation, by an exponential decay law [13]. Moreover, we can observe that its shape does not strongly depend on the walking pattern.

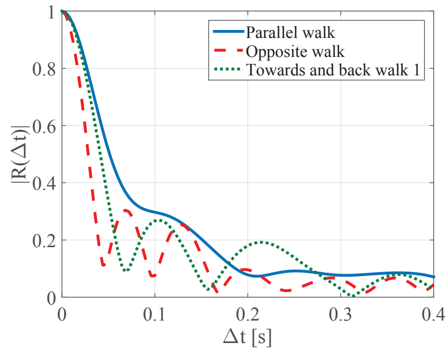

Fig. 3. ACF of normalized transfer function

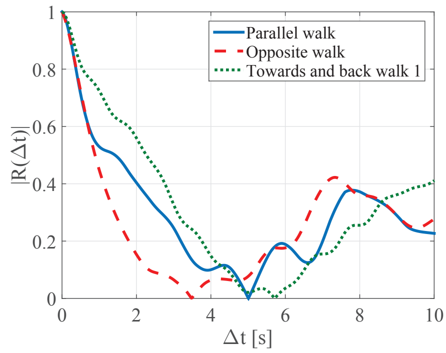

Fig. 4. ACF of long-term fading component

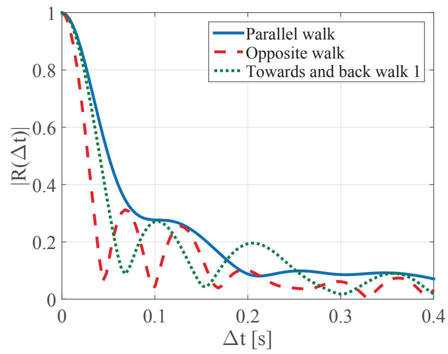

Fig. 5. ACF of short-term fading component

This derives by the fact that long-term fading is mainly due to furniture in the environment and shadowing given by nearby bodies poorly affect the correlation.

Moreover, the short-term fading and channel transfer function ACFs present shapes that are significantly dependent on the type of movement considered. These shapes suggest a behavior that can be described with a combination of Bessel functions as described in [8]. The measured coherence time varies between 29.2 and 34.7 ms. This results, when compared to the coherence time of the long-term fading (typically higher than 500 ms), suggests that the similarities in terms of coherence time and shape of the curves mean that ACF of the transfer function mainly depends on the one of short-term

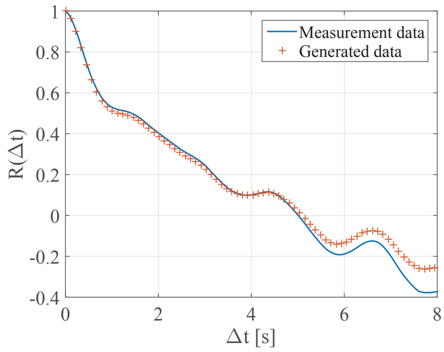

Fig. 6. Long-term fading ACF: measured (blue), generated (red)

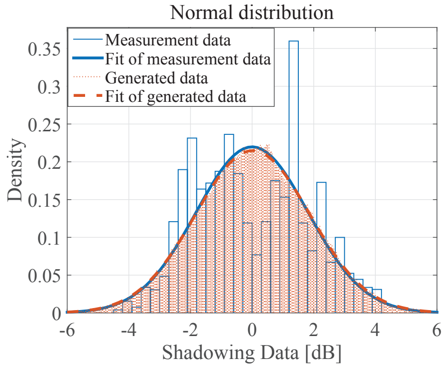

Fig. 7. Long-term fading amplitude distribution: measured (blue), generated (red)

fading. Moreover, the phase information plays an important role in the fast decorrelation of short-term fading [14].

B. Channel Model Implementation Including Time Correlation

Here, we shortly present the results of a channel model implementation including the time correlation properties obtained from measurements. The method is based on the implementation of correlated random normal variables, whose correlation characteristics are retrieved from the measured ACFs previously presented. A classical way to generate a correlated normal distributed random variable with a given correlation matrix $\mathbf{R}$ is done by finding a matrix $\mathbf{U}$ such that:

$$\mathbf{R} = \mathbf{U}\mathbf{U}^{\mathbf{T}} \tag{4}$$

Using this matrix, one can generate correlated random numbers $\mathbf{X_c}$ from uncorrelated standard normal values $\mathbf{X}$ by multiplying them with the aforementioned matrix:

$$\mathbf{X_c} = \mathbf{U}\mathbf{X} \tag{5}$$

Here, we used the Cholesky decomposition of the correlation matrix, a symmetric Toeplitz matrix, in order to calculate $\mathbf{U}$ [12], and obtain a correlated normal random variable.

This method is straightforwardly applied for the long-term fading, since it can be described as normal random variable in dB. Then, the correlated long-term fading, in dB, is obtained by taking into account the measured standard deviation σ_{LT} as follow:

$$\mathbf{S} = \sigma_{LT}\mathbf{X_c} \tag{6}$$

Fig. 6 and Fig. 7 compare the measurement results in parallel walk scenario with those simulated with our implementation in the same scenario. It can be seen that both ACF and amplitude characteristics are in line with the measurement results.

Short-term fading implementation is obtained in a similar manner, by generating normally distributed correlated complex numbers $\mathbf{X_c}$, instead of real values. Therefore, the short-term fading will result from the envelope of $X_{ST} = \sigma_{ST}X_C + b$, where σ_{ST} and b are the measured standard deviation and the root mean square of the dominant component power as defined in [15] respectively. Fig. 8 and Fig. 9 show a comparison

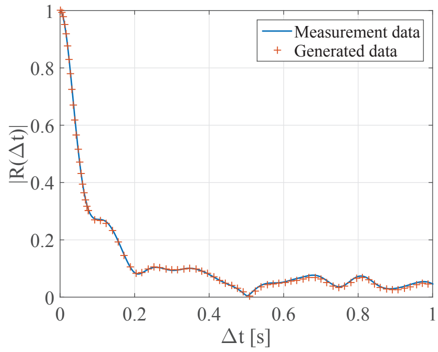

Fig. 8. Short-term fading ACF: measured (blue), generated (red)

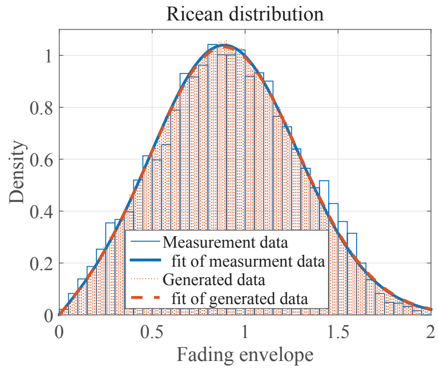

Fig. 9. Short-term fading amplitude distribution: measured (blue), generated (red)

of first and second statistical orders for short-term fading in parallel walk between the measurement data and the data generated with the proposed method. As we can see, an excellent agreement between the measured and the generated data is obtained, thus the method can be implemented in order to generate a stochastic process that has the same statistical properties of the measured data.

IV. Conclusion

The results of a Mobile-to-Mobile channel measurement campaign in indoor environment were exploited to extract the time correlation properties for different pedestrian mobility patterns. The correlation properties of the channel transfer function, as well as those of short- and long-term fading were analyzed.

It was shown that time correlation should be analyzed considering the specific pattern mobility. We pointed out that short-term fading has a predominant effect over the long-term fading. Considering an average speed of 0.5 m/s typical channel coherence time are around 30 ms, while the long-term fading one is between 0.5 and 1 s. These measurement results can be exploited to implement a channel model based on Cholesky factorization, to preserve the second order statistics. The ACF curves shown here suggest an analytical description given by an exponential decay for long-term fading and a combination of Bessel function for the short-term fading. This will be the subject of investigation in future works.

Acknowledgment

This publication was made possible by NPRP grant #[6-1508-2-616] from the Qatar National Research Fund (a member of Qatar Foundation). This work was also partially funded by the Interuniversity Attraction Poles Programme 7/23 BEST-COM initiated by the Belgian Science Policy Office. The statements made herein are solely the responsibility of the authors.

References

[1] M. Gan, N. Czink, P. Castiglione, C. Oestges, F. Tufvesson, and T. Zemen, "Modeling time-variant fast fading statistics of mobile peer-to-peer radio channels," in *Vehicular Technology Conference (VTC Spring), 2011 IEEE 73rd*, May 2011, pp. 1–5.

[2] C. Oestges, N. Czink, B. Bandemer, P. Castiglione, F. Kaltenberger, and A. Paulraj, "Experimental characterization and modeling of outdoor-to-indoor and indoor-to-indoor distributed channels," *Vehicular Technology, IEEE Transactions on*, vol. 59, no. 5, pp. 2253–2265, Jun 2010.

[3] Y. Wang, I. Bonev, J. Nielsen, I. Kovacs, and G. Pedersen, "Characterization of the indoor multiantenna body-to-body radio channel," *Antennas and Propagation, IEEE Transactions on*, vol. 57, no. 4, pp. 972–979, April 2009.

[4] R. Rosini, R. Verdone, and R. D'Errico, "Body-to-body indoor channel modeling at 2.45 ghz," *Antennas and Propagation, IEEE Transactions on*, vol. 62, no. 11, pp. 5807–5819, Nov 2014.

[5] S. Cotton and W. Scanlon, "Channel characterization for single- and multiple-antenna wearable systems used for indoor body-to-body communications," *Antennas and Propagation, IEEE Transactions on*, vol. 57, no. 4, pp. 980–990, April 2009.

[6] M. Olama, S. Djouadi, and C. Charalambous, "Stochastic differential equations for modeling, estimation and identification of mobile-to-mobile communication channels," *Wireless Communications, IEEE Transactions on*, vol. 8, no. 4, pp. 1754–1763, April 2009.

[7] A. Akki and F. Haber, "A statistical model of mobile-to-mobile land communication channel," *Vehicular Technology, IEEE Transactions on*, vol. 35, no. 1, pp. 2–7, Feb 1986.

[8] P. Samarasinghe, T. A. Lamahewa, T. Abhayapala, and R. Kennedy, "2d mobile-to-mobile wireless channel model," in *Signal Processing and Communication Systems (ICSPCS), 2010 4th International Conference on*, Dec 2010, pp. 1–6.

[9] A. Borhani and M. Patzold, "Correlation and spectral properties of vehicle-to-vehicle channels in the presence of moving scatterers," *Vehicular Technology, IEEE Transactions on*, vol. 62, no. 9, pp. 4228–4239, Nov 2013.

[10] F. Mani and R. D'Errico, "Short term fading spatial dependence in indoor body-to-body communications," in *Personal, Indoor, and Mobile Radio Communication (PIMRC), 2015 IEEE 26th Annual International Symposium on*, 2015, pp. 1–5.

[11] ——, "A spatially aware channel model for body to body communications," *submitted to Antennas and Propagation, IEEE Transactions on*, pp. 1–7, 2015.

[12] A. Leon-Garcia, "Probability, statistics and random processes for electrical engineering," 2008.

[13] M. Gudmundson, "Correlation model for shadow fading in mobile radio systems," *Electronics Letters*, vol. 27, no. 23, pp. 2145–2146, Nov 1991.

[14] E. Mondre, "Complex and envelope covariance for rician fading communication channels," *Communication Technology, IEEE Transactions on*, vol. 19, no. 1, pp. 80–84, February 1971.

[15] M. Daoud Yacoub, "Fading distributions and co-channel interference in wireless systems," *Antennas and Propagation Magazine, IEEE*, vol. 42, no. 1, pp. 150–160, Feb 2000.